Robust Subspace Approaches for Analyzing Incomplete Synchrophasor Measurements

Seung-Jun Kim * **Young-hwan Lee** * **Kwang Y. Lee** **

* *Dept. of Computer Science and Electrical Engineering*
University of Maryland, Baltimore County, Baltimore, MD 21250
(e-mail: {sjkim,lee43}@umbc.edu)
** *Dept. of Electrical and Computer Engineering*
Baylor University, Waco, TX 76798
(e-mail: Kwang_Y_Lee@baylor.edu)

Abstract: Synchrophasor measurements can significantly enhance the monitorability of the power grid by revealing the dynamics of grid operation. However, due to high-rate samples collected in large volume, big data challenges emerge to efficiently process the data. The present work advocates robust subspace approaches including robust principal component analysis and subspace clustering, to identify low-dimensional structures in the synchrophasor data, even when portions of measurements are missing due to sensor or network issues, and outliers are present in the data. The outliers can model abnormal dynamics or cyber-attacks in the grid. Numerical tests using simulated synchrophasor data illustrate the utility of the approaches.

Keywords: Synchrophasor, phasor measurement unit, event detection, principal component analysis, subspace clustering, robust techniques, incomplete data, low rank representations.

1. INTRODUCTION

Power system monitoring is a critical task to ensure reliability and efficiency of system operation. Failure to identify abnormalities in the grid states in a timely manner could result in inefficient use of resources, damages to system components, even system instabilities and cascade blackouts. As collection and analysis of large-scale power system data become prevalent, detection and prevention of cyber-attacks via continuous monitoring are essential. Furthermore, as volatile and distributed energy resources are incorporated into future smart grid with increasingly thinner margins of operation, careful real-time monitoring is getting more important than ever.

Recently, the benefit of employing synchrophasor measurements for power system monitoring has been widely recognized (Ree et al. (2010)). Phasor measurement unit (PMU) is a device capable of measuring voltage phasors at each bus at a rate of 30 samples per second or higher. Based on the global positioning system (GPS), multiple PMUs deployed across a wide area can achieve precise synchronization. Compared to the conventional supervisory control and data acquisition (SCADA) architecture, which can provide only few samples in a minute, the synchrophasor measurements can reveal the dynamics of the power system. Thus, the use of PMU data can significantly improve the capability of power system monitoring, protection and control.

However, there are also challenges associated with incorporating PMU data. The large volume of the measurements generated requires significant compression without losing the informative features in the data. Furthermore, the streaming data have to be processed in real time, which may incur heavy computational burden. Based on the data, fast and accurate inference must be performed to detect abnormalities and salient events occurring in the grid. Also, as the data volume grows large, it is plausible to have missing entries in the data, due to various reasons such as sensor failure and errors or congestion in the communication network. The measurements can also be corrupted due to cyber-attack. To perform the data analysis reliably, the missing and corrupt entries must be handled appropriately.

The problem of dimensionality reduction of PMU data was tackled via principal component analysis (PCA) in Dahal et al. (2012) and Chen et al. (2014). The PCA was employed as a preprocessing method for subsequent data analysis and storage in Dahal et al. (2012). The principal components of reduced dimensionality was shown to sufficiently capture the differences between the events with and without frequency oscillations in Chen et al. (2014). Voltage stability of power system was studied in a data-driven manner using the singular value decomposition (SVD) of PMU data in Lim and DeMarco (2013).

The focus of this paper is on resolving missing and corrupt measurements, as well as detecting important events such as topology changes. Data-driven analysis techniques are advocated to identify low-dimensional structure in PMU measurements. Based on spatial and temporal correlations inherent in the data, missing measurements are filled, and corrupt entries corrected. Abnormalities in the system can also be detected by searching for the patterns that deviate from the identified low-dimensional structure.

Missing PMU measurements were reconstructed using low-rank matrix completion approaches in Gao et al. (2014).

Decentralized joint bad data identification and power system state estimation was proposed in Kekatos and Giannakis (2013). Data substitution attack unobservable in the space domain was detected based on temporal correlation in Wang et al. (2014). An event detection algorithm based on PCA was developed in Xie et al. (2014). The distance of the measurement to the low-dimensional subspace was monitored and an event was declared if the distance exceeded a threshold.

Our goal is to incorporate robustness to bad data or abrupt changes in system states, while completing any missing measurements. Two major approaches are considered for this purpose. First, robust PCA is adopted to estimate a low-dimensional subspace in the presence of sparse outliers (Candes et al. (2011)). The outliers capture both corrupt measurements and significant changes in the system states. Secondly, a robust subspace clustering approach is explored (Vidal (2011), Liu et al. (2013), Vidal and Favaro (2014)). The technique is suitable when data points lie in a union of multiple subspaces, rather than a single subspace. The PMU data capturing abrupt changes in system states typically contain multiple subspaces corresponding to pre- and post-event states. Therefore, subspace clustering-based models are well-motivated in this case, and can potentially achieve better dimensionality reduction and inference.

The rest of the paper is organized as follows. In Section 2, the robust PCA algorithm is proposed for completion of missing data under sparse events. Robust subspace clustering for event detection using incomplete data is discussed in Section 3. Results from numerical tests based on synthetic PMU data are presented in Section 4. Conclusion and further research directions are provided in Section 5.

2. ROBUST PCA WITH INCOMPLETE DATA

Consider a PMU dataset collected from N buses over T sampling instants. For simplicity of exposition, only one modality (e.g., the voltage magnitude) of PMU measurements is considered. The dataset can be represented by a matrix $\mathbf{Z} \in \mathbb{R}^{N\times T}$. As both the size of network and the number of samples grow large, collecting a complete set of measurements in $\mathbf{Z}$ is nontrivial, and it is natural to assume that a portion of the entries in $\mathbf{Z}$ may be missing. Let $\Omega \subset \{(n,t) : n \in \{1,2,\ldots,N\},\ t \in \{1,2,\ldots,T\}\}$ denote the set of indices of the entries in $\mathbf{Z}$ that have been collected. Then, operator $\mathcal{P}_\Omega(\mathbf{Z})$ simply sets the missing entries in $\mathbf{Z}$ (that is, the entries whose indices are in Ω^c) to zero, while keeping the rest intact. In other words, upon denoting the (n,t)-entries of $\mathcal{P}_\Omega(\mathbf{Z})$ and $\mathbf{Z}$ as $[\mathcal{P}_\Omega(\mathbf{Z})]_{n,t}$ and $Z_{n,t}$, respectively,

$$[\mathcal{P}_\Omega(\mathbf{Z})]_{n,t} := \begin{cases} Z_{n,t} & \text{if } (n,t) \in \Omega \\ 0 & \text{if } (n,t) \in \Omega^c. \end{cases} \tag{1}$$

The PCA postulates that the data points (the columns of $\mathbf{Z}$) lie in a subspace whose dimension r is lower than the ambient dimension N of the data. This translates to the rank of $\mathbf{Z}$ equal to r. Based on this property, matrix completion techniques have been developed to fill in missing entries in the matrix data. A representative formulation is to minimize a convex surrogate of the rank (which is nonconvex, and thus hard to optimize), subject to the constraints to respect the available data.

$$\min_{\mathbf{X}\in\mathbb{R}^{N\times T}} \|\mathbf{X}\|_* \tag{2a}$$

$$\text{subject to } \mathcal{P}_\Omega(\mathbf{X}) = \mathcal{P}_\Omega(\mathbf{Z}) \tag{2b}$$

where $\mathbf{X}$ is the matrix with the missing entries reconstructed from $\mathcal{P}_\Omega(\mathbf{Z})$, and $\|\mathbf{X}\|_*$ denotes the nuclear norm of $\mathbf{X}$, which is equal to the sum of singular values of $\mathbf{X}$. Minimizing $\|\mathbf{X}\|_*$ encourages the rank of $\mathbf{X}$ to be small (Recht et al. (2010)).

However, the PCA is quite sensitive to outliers or large noise corrupting the measurements. Based on the reasonable assumption that the outliers are rare, the robust PCA (RPCA) thus tries to mitigate the effect of the outliers by introducing a sparse matrix $\mathbf{E}$ (Candes et al. (2011)). With incomplete data, a relevant formulation is

$$\min_{\mathbf{X},\mathbf{E}\in\mathbb{R}^{N\times T}} \|\mathbf{X}\|_* + \lambda\|\mathbf{E}\|_1 \tag{3a}$$

$$\text{subject to } \mathcal{P}_\Omega(\mathbf{Z}-\mathbf{X}-\mathbf{E}) = \mathbf{0} \tag{3b}$$

where $\|\cdot\|_1$ is the ℓ_1-norm, which is equal to the sum of absolute values of the entries in $\mathbf{E}$. The ℓ_1-norm-based penalty as (3a) promotes sparsity in $\mathbf{E}$, i.e., most of the entries in $\mathbf{E}$ are zero. Parameter $\lambda \geq 0$ tunes how sparse $\mathbf{E}$ is. The idea is that the data points that lie outside the nominal low-rank component $\mathbf{X}$ are captured by the sparse component $\mathbf{E}$.

Table 1. RPCA with incomplete data.

Input: Ω, $\mathcal{P}_\Omega(\mathbf{Z})$, $\lambda \geq 0$, $\mu_0 > 0$, μ_{max}, $\rho > 0$, $tol > 0$
Output: $\mathbf{X}$ and $\mathbf{E}$.

1: Initialize $\mathbf{X}_0 = \mathbf{E}_0 = \mathbf{Y}_0 = \mathbf{0}$, $k = 0$
2: While not converged
3: Perform SVD: $\mathcal{P}_\Omega(\mathbf{Z}) - \mathbf{E}_k + \mathbf{Y}_k/\mu_k = \mathbf{U}\mathbf{\Sigma}\mathbf{V}^T$
4: $\mathbf{X}_{k+1} = \mathbf{U}\max\{\mathbf{\Sigma} - \mu_k^{-1}\mathbf{I}, \mathbf{0}\}\mathbf{V}^T$
5: $\mathbf{E}_{k+1}|_\Omega = S_{\lambda/\mu_k}\left((\mathbf{Z} - \mathbf{X}_{k+1} + \mathbf{Y}_k/\mu_k)|_\Omega\right)$
$\mathbf{E}_{k+1}|_{\Omega^c} = (-\mathbf{X}_{k+1} + \mathbf{Y}_k/\mu_k)|_{\Omega^c}$
6: $\mathbf{Y}_{k+1} = \mathbf{Y}_k + \mu_k(\mathcal{P}_\Omega(\mathbf{Z}) - \mathbf{X}_{k+1} - \mathbf{E}_{k+1})$
7: $\mu_{k+1} = \min\{\rho\mu_k, \mu_{max}\}$
8: Check $\|\mathcal{P}_\Omega(\mathbf{Z}) - \mathbf{X}_{k+1} - \mathbf{E}_{k+1}\|_F < tol$
9: $k \leftarrow k+1$
10: End while
11: Set $\mathbf{X} = \mathbf{X}_k$, $\mathbf{E}|_\Omega = \mathbf{E}_k|_\Omega$, and $\mathbf{E}|_{\Omega^c} = \mathbf{0}$.

Although (3) is a convex optimization problem, which can be solved for a globally optimal solution using generic convex optimization software, tailored algorithms often provide better performance in terms of accuracy and computational cost. Two iterative algorithms for (3) were derived in Shang et al. (2014). One of the algorithms is reproduced in Table 1 for completeness. The soft thresholding operator $S_\eta(\cdot)$ used in Table 1 is defined as

$$S_\eta(x) := \max\{0, |x| - \eta\}\text{sgn}(x) \tag{4}$$

and $S_\eta(\mathbf{X})$ for matrix $\mathbf{X}$ applies the operation elementwise. $\mathbf{X}|_\Omega$ refers to the entries of $\mathbf{X}$ whose indices are in Ω. Parameters μ_0, μ_{max} and ρ determine the sequence of step sizes $\{\mu_k\}$ through line 7. The step size sequence typically affect the convergence speed.

Once the algorithm has converged, $\mathbf{X}$ has a rank r, which is much smaller than N. The basis for the r-dimensional subspace is given by the r columns of $\mathbf{U}$ corresponding to the r largest singular values, and the principal components are the r rows of $\max\{\mathbf{\Sigma} - \mu_k^{-1}\mathbf{I}, \mathbf{0}\}\mathbf{V}^T$ corresponding to the same set of singular values; cf. line 4 in Table 1. Thus,

small r can yield significant dimensionality reduction of the PMU data. Missing entries in $\mathbf{Z}$ are also recovered based on the subspace structure. Moreover, non-zero entries in $\mathbf{E}$ indicate that the corresponding entries in $\mathbf{Z}$ significantly deviate from the nominal subspace structure, which may imply abnormalities or cyber-attacks in the system.

3. ROBUST SUBSPACE CLUSTERING WITH INCOMPLETE DATA

The PCA approach postulates that there is a single subspace to which all data points belong. When the power system undergoes significant changes in operating states due to, say, sudden alteration in the topology or renewable generation outputs, the single subspace model may be no longer suitable. A slightly rich model is a subspace clustering model, where the data are postulated to lie in a union of more than one subspace.

Thus, the goal of subspace clustering is to identify the number and bases of salient subspaces in the dataset, and cluster (assign) the individual data points into one of the subspaces. Suppose a set of data points $\{\mathbf{z}_t \in \mathbb{R}^N\}_{t=1}^T$ are available. For now, no missing entries are assumed in vectors $\{\mathbf{z}_t\}$. Let w_{ti} be a binary variable equal to 1 if the t-th datum is assigned to the i-th cluster, and 0 otherwise. Assuming that the number of clusters K is fixed, one can formulate the subspace clustering problem as

$$\min_{\{\mathbf{U}_i\},\{\mathbf{y}_t\},\{w_{ti}\}} \sum_{t=1}^{T}\sum_{i=1}^{K} w_{ti}\|\mathbf{z}_t - \mathbf{U}_i\mathbf{y}_t\|_2^2 \tag{5a}$$

$$\text{subject to } w_{ti} \in \{1,0\}\ \forall i,t \text{ and } \sum_{i=1}^{K} w_{ti} = 1\ \forall t \tag{5b}$$

An intuitive approach to achieve this is to alternate between subspace estimation and clustering. That is, given the cluster assignments $\{w_{ti}\}$, the basis vectors $\mathbf{U}_i$ for the points assigned to the i-th cluster can be obtained by PCA. Given $\{\mathbf{U}_i\}$, individual data points can then be assigned to the closest subspace, yielding updated $\{w_{ti}\}$. Repeating this process yields a locally optimal solution for (5).

There has been a host of approaches to solve the subspace clustering problem (Vidal (2011)). The focus of this work is to develop a subspace clustering algorithm for incomplete data that also contain outliers, and test its performance on PMU data. Our novel algorithm is based on low-rank-based subspace clustering (Liu et al. (2013), Vidal and Favaro (2014)). The basic formulation is

$$\min_{\mathbf{C}} \|\mathbf{C}\|_* \tag{6a}$$

$$\text{subject to } \mathbf{Z} = \mathbf{Z}\mathbf{C}. \tag{6b}$$

It was shown in Liu et al. (2013) that the solution to (6) is given by $\mathbf{V}_0\mathbf{V}_0^T$, where $\mathbf{Z} = \mathbf{U}_0\mathbf{\Sigma}_0\mathbf{V}_0^T$ is the skinny SVD of $\mathbf{Z}$. When the data points $\mathbf{Z}$ lie exactly in a union of independent subspaces, it can be shown that $\mathbf{V}_0\mathbf{V}_0^T$ forms a block diagonal matrix such that the (t,t')-th entry is nonzero only if the t-th and the t'-th samples belong to the same subspaces (Kanatani (2001)). Thus, $\mathbf{C}$ can be used as an affinity matrix for performing clustering through, e.g., spectral clustering (Luxburg (2007)).

The noise and outliers corrupting the measurements can be handled in this context by relaxing the constraint (6b) and introducing a sparse matrix $\mathbf{E}$ (Vidal and Favaro (2014)). To incorporate the incomplete data as well, the following formulation is considered.

$$\min_{\mathbf{X},\mathbf{C},\mathbf{E}} \|\mathbf{C}\|_* + \frac{\tau}{2}\|\mathbf{X} - \mathbf{X}\mathbf{C}\|_F^2 + \lambda\|\mathbf{E}\|_1 \tag{7a}$$

$$\text{subject to } \mathcal{P}_\Omega(\mathbf{Z} - \mathbf{X} - \mathbf{E}) = \mathbf{0},\ \mathbf{C} = \mathbf{C}^T \tag{7b}$$

where $\mathbf{X}$ is the reconstructed data matrix based on the union-of-subspaces structure, $\tau \geq 0$ tunes the severity of enforcing the structure in $\mathbf{X}$, and $\lambda \geq 0$ adjusts the severity of the sparsity penalty. Constraint $\mathbf{C} = \mathbf{C}^T$ is motivated by the interpretation of $\mathbf{C}$ as $\mathbf{V}_0\mathbf{V}_0^T$ in the noiseless case.

To derive an iterative algorithm for solving (7), it is first noted that $\mathbf{E}|_{\Omega^c} = \mathbf{0}$ at the optimum. Thus, (7) is equivalent to

$$\min_{\mathbf{X},\mathbf{C},\mathbf{E}} \|\mathbf{C}\|_* + \frac{\tau}{2}\|\mathbf{X} - \mathbf{X}\mathbf{C}\|_F^2 + \lambda\|\mathcal{P}_\Omega(\mathbf{E})\|_1 \tag{8a}$$

$$\text{subject to } \mathcal{P}_\Omega(\mathbf{Z}) = \mathbf{X} + \mathbf{E} \tag{8b}$$

$$\mathbf{C} = \mathbf{C}^T. \tag{8c}$$

Our approach to solve this problem is to adopt the alternating direction method of multipliers (ADMM), which is useful for decomposing hard optimization problems with coupled variables into easily solvable subproblems in individual variables (Boyd et al. (2011)). First, upon introducing a Lagrange multiplier matrix $\mathbf{Y}$ associated with (8b), the augmented Lagrangian is constructed as

$$L_\mu(\mathbf{X},\mathbf{C},\mathbf{E};\mathbf{Y}) = \|\mathbf{C}\|_* + \frac{\tau}{2}\|\mathbf{X} - \mathbf{X}\mathbf{C}\|_F^2 + \lambda\|\mathcal{P}_\Omega(\mathbf{E})\|_1 + \langle\mathbf{Y}, \mathcal{P}_\Omega(\mathbf{Z}) - \mathbf{X} - \mathbf{E}\rangle + \frac{\mu}{2}\|\mathcal{P}_\Omega(\mathbf{Z}) - \mathbf{X} - \mathbf{E}\|_F^2. \tag{9}$$

Then, the ADMM produces iterative update rules for $\mathbf{X}_k$, $\mathbf{C}_k$, $\mathbf{E}_k$, and $\mathbf{Y}_k$ at iteration k as

$$\mathbf{X}_{k+1}, \mathbf{C}_{k+1} = \arg\min_{\mathbf{X},\mathbf{C}:\mathbf{C}=\mathbf{C}^T} L_{\mu_k}(\mathbf{X},\mathbf{C},\mathbf{E}_k;\mathbf{Y}_k) \tag{10}$$

$$\mathbf{E}_{k+1} = \arg\min_{\mathbf{E}} L_{\mu_k}(\mathbf{X}_{k+1},\mathbf{C}_{k+1},\mathbf{E};\mathbf{Y}_k) \tag{11}$$

$$\mathbf{Y}_{k+1} = \mathbf{Y}_k + \mu_k(\mathcal{P}_\Omega(\mathbf{Z}) - \mathbf{X}_{k+1} - \mathbf{E}_{k+1}). \tag{12}$$

The optimization problem associated with the update for $\mathbf{X}$ and $\mathbf{C}$ in (10) can be written as

$$\min_{\mathbf{X},\mathbf{C}:\mathbf{C}=\mathbf{C}^T} \|\mathbf{C}\|_* + \frac{\tau}{2}\|\mathbf{X} - \mathbf{X}\mathbf{C}\|_F^2 + \frac{\mu_k}{2}\|\mathcal{P}_\Omega(\mathbf{Z}) - \mathbf{X} - \mathbf{E}_k + {\mu_k}^{-1}\mathbf{Y}_k\|_F^2 \tag{13}$$

which is essentially Problem (P_3) in Vidal and Favaro (2014), for which a closed-form solution can be derived. Specifically, let the SVD of $\mathcal{P}_\Omega(\mathbf{Z}) - \mathbf{E}_k + \mu_k^{-1}\mathbf{Y}_k$ be computed as $\mathbf{U}_1\mathbf{\Sigma}_1\mathbf{V}_1^T$ and σ_n be the n-th diagonal entry in $\mathbf{\Sigma}_1$. Then, s_n is obtained as the solution s to

$$\sigma_n = \psi(s) := \begin{cases} s + \dfrac{1}{\mu_k\tau}s^{-3} & \text{if } s > \dfrac{1}{\sqrt{\tau}} \\ s + \dfrac{\tau}{\mu_k}s & \text{if } s \leq \dfrac{1}{\sqrt{\tau}} \end{cases} \tag{14}$$

and $\mathbf{S} := \text{diag}(s_1,\ldots,s_N)$. Define also

$$P_\tau(s) := \begin{cases} 1 - \dfrac{1}{\tau s^2} & \text{if } s > \dfrac{1}{\sqrt{\tau}} \\ 0 & \text{if } s \leq \dfrac{1}{\sqrt{\tau}} \end{cases}. \tag{15}$$

Then, the optimal solution to (13) is given by $\mathbf{X}_{k+1} = \mathbf{U}_1\mathbf{S}\mathbf{V}_1^T$ and $\mathbf{C}_{k+1} = \mathbf{V}P_\tau(\mathbf{S})\mathbf{V}^T$.

Table 2. RSC with incomplete data.

Input: Ω, $\mathcal{P}_\Omega(\mathbf{Z})$, $\tau \geq 0$, $\lambda \geq 0$, $\mu_0 > 0$, μ_{max}, $\rho > 0$, $tol > 0$
Output: $\mathbf{X}$, $\mathbf{C}$, and $\mathbf{E}$.

1: Initialize $\mathbf{X}_0$, $\mathbf{C}_0$, $\mathbf{E}_0$ and $\mathbf{Y}_0$. Set $k = 0$
2: While not converged
3: Perform SVD: $\mathcal{P}(\mathbf{Z}) - \mathbf{E}_k + \mathbf{Y}/\mu_k = \mathbf{U}_1\mathbf{\Sigma}_1\mathbf{V}_1^T$
4: $\mathbf{X}_{k+1} = \mathbf{U}_1\mathbf{S}\mathbf{V}_1^T$ with $\mathbf{S}$ computed via (14)
5: $\mathbf{E}_{k+1}|_\Omega = S_{\lambda/\mu_k}\left((\mathbf{Z} - \mathbf{X}_{k+1} + \mathbf{Y}_k/\mu_k)|_\Omega\right)$
$\mathbf{E}_{k+1}|_{\Omega^c} = (-\mathbf{X}_{k+1} + \mathbf{Y}_k/\mu_k)|_{\Omega^c}$
6: $\mathbf{Y}_{k+1} = \mathbf{Y}_k + \mu_k(\mathcal{P}_\Omega(\mathbf{Z}) - \mathbf{X}_{k+1} - \mathbf{E}_{k+1})$
7: $\mu_{k+1} = \min\{\rho\mu_k, \mu_{max}\}$
8: Check $\|\mathcal{P}_\Omega(\mathbf{Z}) - \mathbf{X}_{k+1} - \mathbf{E}_{k+1}\|_F < tol$
9: $k \leftarrow k + 1$
10: End while
11: Set $\mathbf{X} = \mathbf{X}_k$, $\mathbf{C} = \mathbf{V}_1 P_\tau(\mathbf{S})\mathbf{V}_1^T$, $\mathbf{E}|_\Omega = \mathbf{E}_k|_\Omega$, $\mathbf{E}|_{\Omega^c} = \mathbf{0}$.

The update in (11) needs to solve

$$\min_{\mathbf{E}} \lambda\|\mathcal{P}_\Omega(\mathbf{E})\|_1 + \frac{\mu_k}{2}\|\mathcal{P}_\Omega(\mathbf{Z}) - \mathbf{X}_{k+1} - \mathbf{E} + \mu_k{}^{-1}\mathbf{Y}_k\|_F^2 \tag{16}$$

whose solution is again given in a closed form by

$$\mathbf{E}_{k+1}|_\Omega = S_{\lambda/\mu_k}\left((\mathbf{Z} - \mathbf{X}_{k+1} + \mu_k^{-1}\mathbf{Y}_k)|_\Omega\right) \tag{17}$$

$$\mathbf{E}_{k+1}|_{\Omega^c} = (-\mathbf{X}_{k+1} + \mu_k^{-1}\mathbf{Y}_k)|_{\Omega^c}. \tag{18}$$

Overall, the iterative algorithm for robust subspace clustering (RSC) for incomplete data is listed in Table 2.

4. NUMERICAL TESTS

To test the effectiveness of the proposed subspace approaches, synthetic PMU data were generated using the PSS/E simulator (Siemens (2013)). The tested grid containing 23 buses and 6 generators is shown in Fig. 1. The dynamic models of the generators adopted for simulation are listed in Table 3.

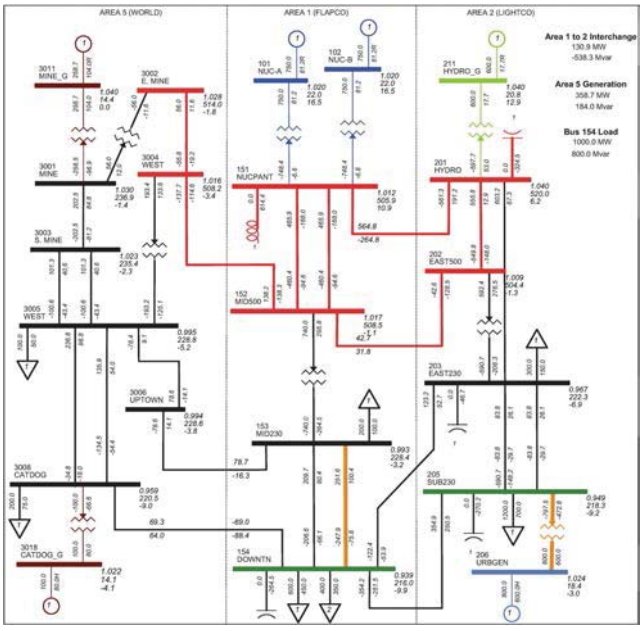

Fig. 1. A 23-bus 6-generator system.

Table 3. Dynamic models of generators.

Bus number	Generator	Exciter	Turbine governor
101	GENROU	IEEET1	TGOV1
102	GENROU	IEEET1	TGOV1
206	GENROU	IEEET1	TGOV1
211	GENSAL	SCRX	HYGOV
3011	GENROU	SEXS	None
3018	GENROU	SEXS	None

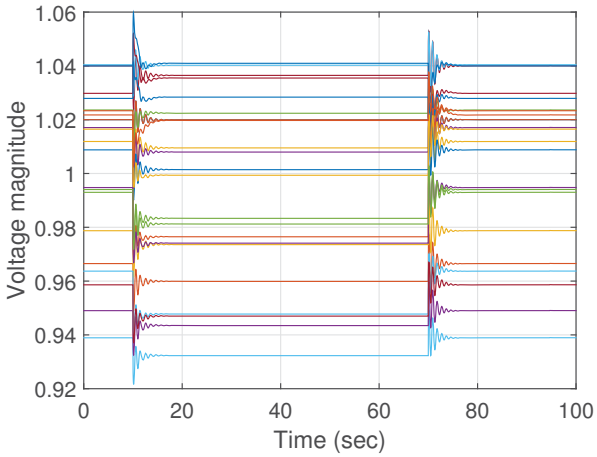

(a)

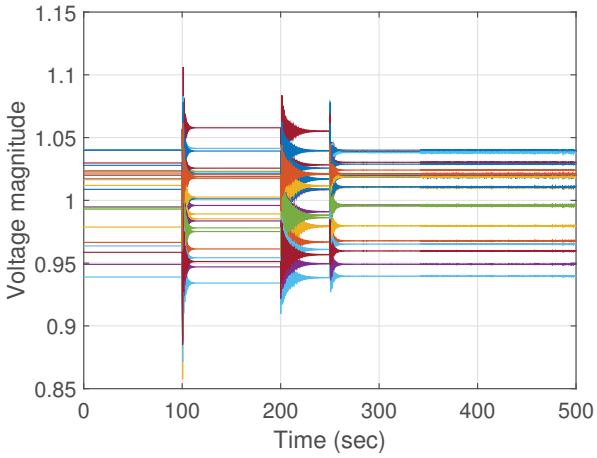

(b)

Fig. 2. Voltage magnitudes. (a) Scenario 1. (b) Scenario 2.

Two scenarios were simulated. In Scenario 1, the transmission line connecting buses 3001 and 3003 is tripped at $t = 10$ sec and then closed at $t = 70$ sec. The corresponding voltage magnitudes at all buses are shown in Fig. 2(a). In Scenario 2, the line connecting buses 151 and 201 is tripped at $t = 100$ sec, followed by a trip of the generator at bus 102 at $t = 200$ sec. Subsequently, the previously tripped line is closed at $t = 250$ sec. The voltage magnitudes for Scenario 2 are plotted in Fig. 2(b).

The events such as the line or the generator trips cause transients to appear in the PMU snapshots, which are outside the nominal subspaces occupied by the measurements in the steady state. Thus, the sparse components intended to capture the outliers in the data can indicate the appearance of those transients, which may be used for detection of salient events in the system.

Fig. 3 shows the sparse component $\mathbf{E}$ from the RPCA and RSC algorithms in the two scenarios tested. Figs. 3(a) and (b) depict $\mathbf{E}$ from the RPCA algorithm, and Figs. 3(c) and (d) from the RSC. The values for λ and τ were

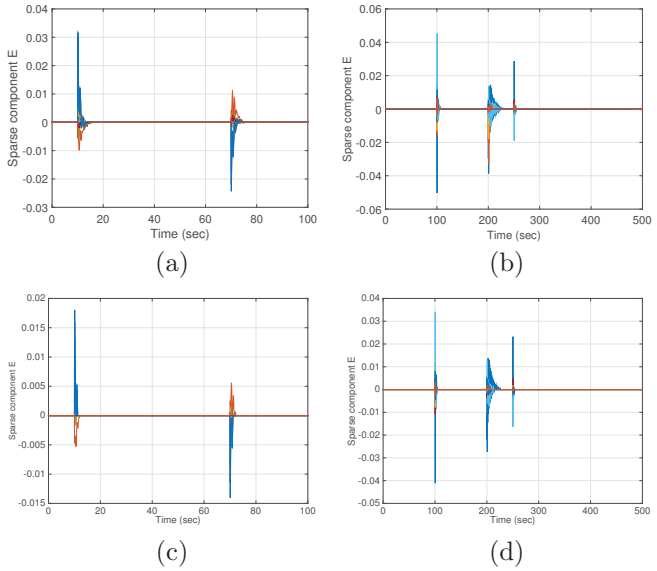

Fig. 3. Sparse component **E**. (a) RPCA for Scenario 1. (b) RPCA for Scenario 2. (c) RSC for Scenario 1. (d) RSC for Scenario 2.

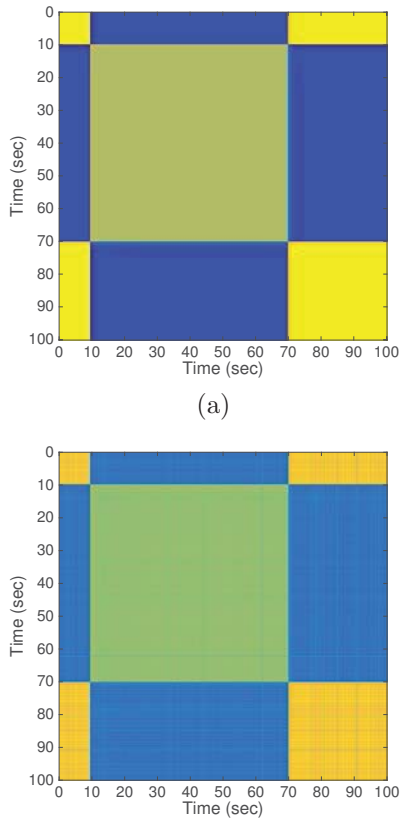

Fig. 4. Matrix **C** from RSC for Scenario 1. (a) With no missing data. (b) With 50% missing data.

set to 0.05 and 20, respectively. It can be seen that the abnormalities due to the events are clearly captured by the nonzero components in **E**. The rank of matrix **X** from RPCA and the rank of **C** from RSC were equal to 13 and 2, respectively, for Scenario 1, and 14 and 3, respectively, for Scenario 2. Thus, RSC achieves the same

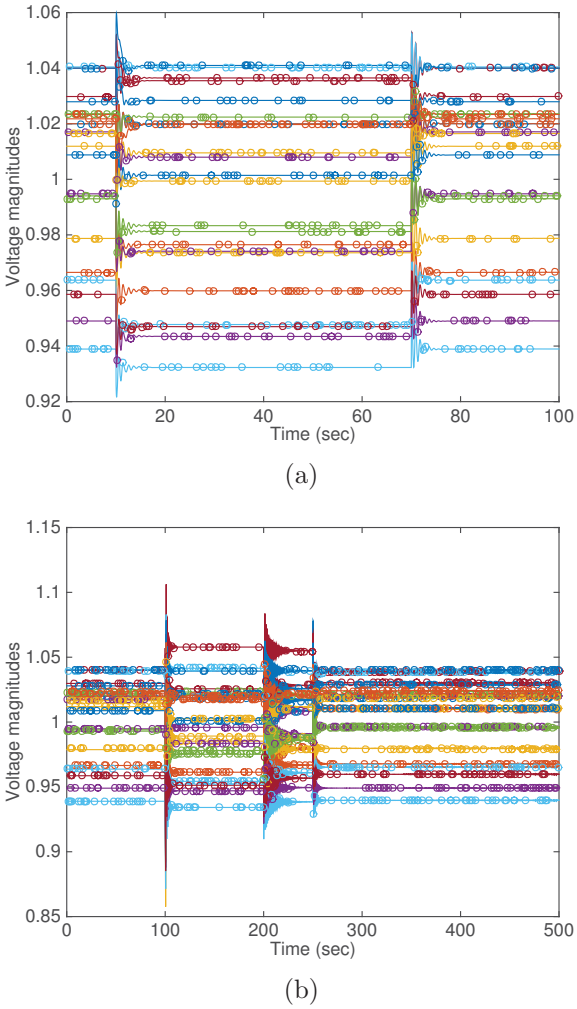

Fig. 5. True and reconstructed voltage magnitudes. (a) Scenario 1 with RPCA. (b) Scenario 2 with RSC.

event detection capability with much larger reduction in the dimensionality, underlining the enhanced modeling capability of the RSC compared to RPCA.

Fig. 4(a) depicts matrix **C** obtained from RSC for Scenario 1. It is clearly seen that the data points before $t = 10$ sec and those after $t = 70$ sec belong to the same subspace, while the points in the middle occupies another subspace.

To assess the capability of the subspace approaches for completing missing PMU measurements, uniformly random entries in matrix **Z** were removed, which were then reconstructed using the proposed algorithms. Fig. 5 shows the true and the reconstructed entries of the voltage magnitudes with 1% misses, where the circles indicate the reconstructed versions of the misses. Fig. 5(a) corresponds to the case of using RPCA for Scenario 1, and Fig. 5(b) RSC for Scenario 2. As the RSC problem is nonconvex, the result is quite sensitive to the initialization. Using **X** from RPCA as the initializer for **X** in RSC yielded a good performance. It can be seen that the reconstructed values are quite accurate, especially in the steady-state regions. The normalized mean square error (MSE) for the missing entries is on the order of 10^{-4}.

Fig. 4(b) depicts matrix $\mathbf{C}$ from RSC for Scenario 1 when 50% of the data are missing. It is clearly seen that the subspace segmentation can be obtained quite robustly.

Fig. 6 depicts the normalized MSE when the proportion of the missing data is varied. Fig. 6(a) corresponds to the error for both the missing and available entries, and Fig. 6(b) depicts the error computed only over the missing part. It can be seen that both RPCA and RSC perform quite comparably and reconstructs the data reliably.

5. CONCLUSION AND FUTURE WORK

The PMU data with missing measurements were analyzed using robust subspace approaches. Robust PCA modeled the PMU data to lie in a single subspace modulo possible sparse outliers. Robust subspace clustering postulated a union of multiple subspaces as the nominal low-dimensional structure. Abrupt changes in the grid topology or the grid state could be captured in the sparse outlier component, which illustrated how the technique could be useful for detecting abnormalities or cyber-attacks in the grid. Missing measurements were seen to be reconstructed from available data based on the low-dimensional model. Compared to RPCA, the RSC approach could achieve comparable event detection and missing data completion performances while significantly reducing the dimensionality of the data. Future research directions include online processing of the data and building event classifiers based on the reduced dimensional features.

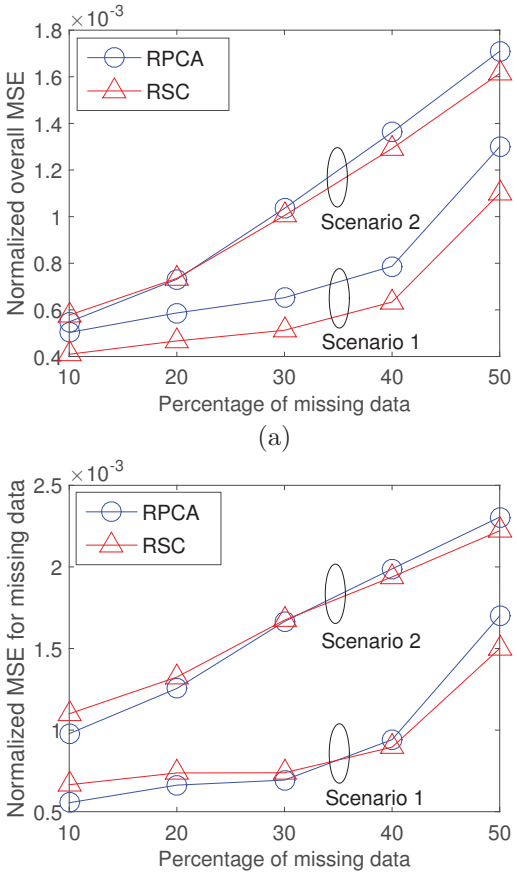

Fig. 6. Normalized MSEs. (a) Overall error. (b) Error over missing entries.

REFERENCES

Boyd, S., Parikh, N., Chu, E., Peleato, B., and Eckstein, J. (2011). Distributed optimization and statistical learning via the alternating direction method of multipliers. *Foundations and Trends in Machine Learning*, 3(1), 1–122.

Candes, E.J., Li, X., Ma, Y., and Wright, J. (2011). Robust principal component analysis? *Journal of the ACM*, 58(3).

Chen, Y., Xie, L., and Kumar, P.R. (2014). Power system event classification via dimensionality reduction of synchrophasor data. In *Proc. of the IEEE 8th Sensor Array and Multichannel Sig. Proc. Workshop*, 57–60. A Coruña, Spain.

Dahal, N., King, R.L., and Madani, V. (2012). Online dimension reduction of synchrophasor data. In *Proc. of the IEEE PES T&D Conf. Expo.*, 1–7. Orlando, FL.

Gao, P., Wang, M., Ghiocel, S.G., and Chow, J.H. (2014). Modeless reconstruction of missing synchrophasor measurements. In *IEEE PES General Meeting*, 1–5. National Harbor, MD.

Kanatani, K. (2001). Motion segmentation by subspace separation and model selection. In *Proc. of the 8th Intl. Conf. Computer Vis.*, 586–591. Vancouver, Canada.

Kekatos, V. and Giannakis, G.B. (2013). Distributed robust power system state estimation. *IEEE Trans. Power Syst.*, 28(2), 1617–1626.

Lim, J.M. and DeMarco, C.L. (2013). Model-free voltage stability assessments via singular value analysis of pmu data. In *Proc. of the IREP Symp. - Bulk Power Syst. Dynamics and Contr. - IX Optimization, Security and Control of the Emerging Power Grid*, 1–10. Rethymno, Greece.

Liu, G., Lin, Z., Yan, S., Sun, J., Yu, Y., and Ma, Y. (2013). Robust recovery of subspace structures by low-rank representation. *IEEE Trans. Pattern Anal. Mach. Intell.*, 35(1), 171–184.

Luxburg, U. (2007). A tutorial on spectral clustering. *Stat. Comput.*, 17, 395–416.

Recht, B., Fazel, M., and Parrilo, P.A. (2010). Guaranteed minimum-rank solutions of linear matrix equations via nuclear norm minimization. *SIAM Rev.*, 52(3), 471–501.

Ree, J.D.L., Centeno, V., Thorp, J.S., and Phadke, A.G. (2010). Synchronized phasor measurement applications in power systems. *IEEE Trans. Smart Grid*, 1(1), 20–27.

Shang, F., Liu, Y., Cheng, J., and Cheng, H. (2014). Robust principal component analysis with missing data. In *Proc. of the 23rd ACM Intl. Conf. Info. Knowl. Mgmt.*, 1149–1158. Shanghai, China.

Siemens (2013). PSS/E Documentation, Version 33.5.

Vidal, R. (2011). Subspace clustering. *IEEE Sig. Proc. Mag.*, 28(2), 52–68.

Vidal, R. and Favaro, P. (2014). Low rank subspace clustering (LRSC). *Patt. Recog. Lett.*, 43, 47–61.

Wang, M., Gao, P., Ghiocel, S.G., Chow, J.H., Fardanesh, B., Stefopoulos, G., and Razanousky, M.P. (2014). Identification of "unobservable" cyber data attacks on power grids. 830–835.

Xie, L., Chen, Y., and Kumar, P.R. (2014). Dimensionality reduction of synchrophasor data for early event detection: Linearized analysis. *IEEE Trans. Power Syst.*, 29(6), 2784–2794.